Z. Phys. D 42, 203–208 (1997)

ZEITSCHRIFT
FÜR PHYSIK D

Experimental determination of deposition induced cluster deformation

H. Hövel*, A. Hilger, I. Nusch, U.Kreibig

I. Physikalisches Institut der RWTH Aachen, Aachen University of Technology, D-52056 Aachen, Germany

Received: 17 February 1997 / Final version: 26 August 1997

Abstract. We describe an experimental method to measure the cluster deformation of metal clusters deposited on a substrate. It is based upon the sensitivity of the cluster plasmon resonance on the geometric shape of the clusters; it uses optical spectroscopy with polarized light in oblique incidence. The proposed method was applied to silver clusters (mean diameter $2R = 2\,nm$) produced in a supersonic beam and deposited on a quartz glass substrate. Cluster deposition and optical measurements were performed in situ in vacuum. At an estimated particle velocity of $1.5 \cdot 10^3\,m\,s^{-1}$, we evaluated an axial ratio of $c/a = 0.86$ for the deposition induced deformation. This result is compared to data from molecular dynamical simulations. By varying the substrate coverage, the critical cluster coverage for the onset of electromagnetic cluster–cluster coupling and coalescence was determined to amount to 0.1 cluster-monolayers.

PACS: 61.46; 36.40; 71.45.Gm; 73.20.Mf

1 Introduction

In several recent studies the "fate" of clusters deposited on solid substrates from a supersonic beam was discussed [1–6]. This was motivated among others by the recent development to produce thin films from clusters instead of atoms, in order to improve film properties [1, 7]. Molecular dynamical simulations of the deposition process [1, 2, 4] proved that rapid clusters are deformed or even destroyed when impinging on the substrate surface. Short-time processes ($t < 10^{-10}s$) in the clusters and the substrate during the impact are driven by the kinetic energy of the clusters. For the long-time restructuration of the clusters the substrate temperature is essential [6] and the interfacial cluster-substrate interaction has important influence on the final cluster shape [8]. In the case of the strong interaction of metal clusters with a metal substrate this can even lead to an almost complete flattening. This effect also depends on the substrate temperature [9]. Hence it is important to measure in situ the cluster shape after the deposition. In the following we describe an optical method to determine quantitatively the shape of metal clusters impinging on arbitrary but transparent substrates.

* *Present address:* Experimentelle Physik I, Universität Dortmund, D-44221 Dortmund, Germany (e-mail: hoevel@physik.uni-dortmund.de)

2 Extinction spectra of cluster systems

The presented method is based upon the sensitivity of the plasmon resonance of metal clusters on their geometric shape. This was tested optically by applying polarized light under grazing incidence. It is restricted to planar transparent substrate surfaces and cluster materials which exibit destinct cluster plasmons. The latter is fulfilled for example for the cluster plasmons of silver, gold, copper and the alkali metals which are situated in the visible spectrum. Aluminium and magnesium show clear cluster plasmons at higher photon energies.

Before discussing the experimental results we give a short survey of the description of optical spectra which are observed for well separated clusters of different shapes and for aggregates of clusters.

2.1 Single spherical clusters

For the experiments presented in the following the cluster diameter is much smaller than the wavelength of the incident light, therefore the quasistatic approximation of the Mie-theory can be used [10, 11]. The optical extinction cross-section of silver clusters with diameters below $15\,nm$ is given merely by dipole absorption and shows the narrow resonance of the cluster plasmon, the peak position ω_1 of which is approximately determined by the condition

$$\varepsilon_1(\omega_1) = -2\varepsilon_m \tag{1}$$

with $\varepsilon(\omega) = \varepsilon_1(\omega) + i\varepsilon_2(\omega)$ and ε_m = const the dielectric functions of the cluster material and of the surrounding medium, respectively. The full half-width of the resonance peak is determined by the imaginary part and also the slope of the real part of the dielectric function at the frequency ω_1 (see [12]).

For small sizes the dielectric function of the cluster material differs from that of the corresponding bulk metal. This can be considered by modelling the cluster size effects in

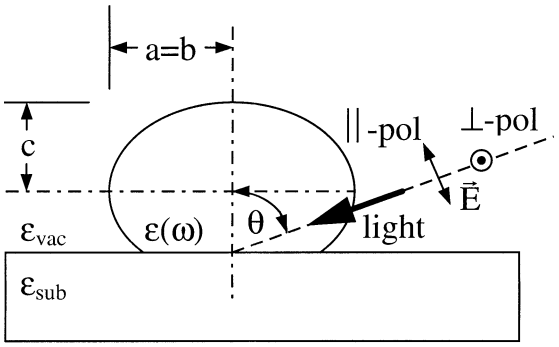

Fig. 1. Truncated spheroidal cluster on a substrate. The geometry of optical extinction measurements with oblique incidence and polarized light is indicated (explanation of symbols: see text)

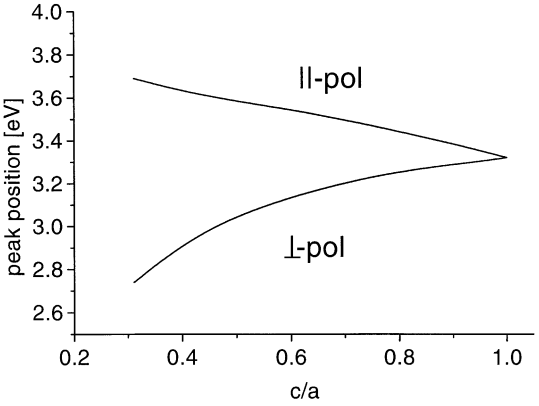

Fig. 2. Peak positions for $\perp$-polarization (σ^a_{abs}) and $\|$-polarization (σ^c_{abs}) calculated for the special example of spheroidal oblate silver clusters on a quartz glass substrate using bulk $\varepsilon(\omega)$ and ε_m = 1.48

$\varepsilon(\omega)$ [11]. In general, both the width and the peak position of the cluster plasmon resonance are influenced. If the clusters are in contact with other material – for example by embedding them in a matrix or depositing them on a substrate or by surrounding absorbates – the correction of $\varepsilon(\omega)$ has to include chemical interface effects. This is described in detail in [12].

2.2 Single nonspherical clusters

Deviations from the spherical shape, as occuring when spherical clusters are deposited with high velocity on a substrate, are causing changes of the optical spectra, which can be approximately described by the dipole absorption of ellipsoids

$$\sigma^i_{abs}(\omega) = \frac{1}{L_i^2}\frac{\omega}{c}\varepsilon_m^{3/2}V_0\frac{\varepsilon_2(\omega)}{[\varepsilon_1(\omega)+\left(1/L_i-1\right)\varepsilon_m]^2+\varepsilon_2(\omega)^2}\,,$$
$$i\epsilon\{a,b,c\}\,. \qquad (2)$$

$V_0 = (4/3)\pi abc$ is the volume of the ellipsoid. The geometrical factors L_a, L_b and L_c determine the resonance positions for the electric field of the incident light parallel to each of the three principal axes a, b and c of the ellipsoid [10, 11]. For a spherical cluster $L_a = L_b = L_c = 1/3$ leads to the peak position given in (1).

A high velocity cluster impinging on a surface is flattened. So we consider the special case of an oblate spheroidal cluster with its major axes in the plane of the substrate (see Fig. 1). In this case it is $c < a$ and

$$L_a = L_b = \frac{g(e)}{2e^2}\left[\frac{\pi}{2} - \arctan g(e)\right] - \frac{g^2(e)}{2}$$
$$L_c = 1 - 2L_a$$
$$\text{with}\quad g(e) = \left(\frac{1-e^2}{e^2}\right)^{1/2} \quad\text{and}\quad e^2 = 1 - \frac{c^2}{a^2}\quad . \qquad (3)$$

Absorption spectra with $\perp$- and $\|$-polarization in oblique incidence are different and can thus be used to determine the axial ratio. The indices $\perp$ and $\|$ correspond to electrical field vectors perpendicular or parallel to the plane of incidence. With θ the angle of incidence it is

$$\sigma^{\perp}_{abs}(\omega)=\sigma^a_{abs}(\omega)$$
$$\sigma^{\|}_{abs}(\omega)=\sigma^a_{abs}(\omega)\cos^2\theta + \sigma^c_{abs}(\omega)\sin^2\theta \quad . \qquad (4)$$

Hence in $\sigma^{\|}_{abs}$ both resonances are mixed. Using grazing incidence we have $\cos^2\theta \approx 0$ and $\sin^2\theta \approx 1$ and this separates the peaks $\sigma^{\perp}_{abs} = \sigma^a_{abs}(\omega)$ and $\sigma^{\|}_{abs} \approx \sigma^c_{abs}(\omega)$. For $\perp$-polarized light the resonance position is determined by the geometrical factor $L_a = L_b < 1/3$. This shifts the resonance position to lower energies compared to a spherical cluster if $(d\varepsilon_1(\omega)/d\omega)_{\omega=\omega_1} > 0$ which is generally the case for metal clusters. For $\|$-polarized light one observes the resonance position corresponding to the minor axis which is perpendicular to the substrate. In this case $L_c > 1/3$ then leads to a shift to higher energies. By fitting experimental spectra by (2) and (4), the L_i can be determined and therefrom via (3) the ratio c/a.

To give an overview we show the resulting peak positions using the model described above for the special case of silver clusters on a quartz glass substrate in Fig. 2. The parameter ε_m = 1.48, which was obtained by fitting the experimental data shown below, includes not only the electromagnetic influence of the substrate, but also the corrections of $\varepsilon(\omega)$ caused by chemical interface effects concerning the peak positions. For the evaluation of the experimental spectra given below we used calculations based upon (2), (3) and (4) including the size and interface dependent $\varepsilon(\omega, R)$ described in [12].

The accuracy of the calculations presented in the following is limited mainly by two approximations:

First, the use of one ε_m in (2) neglects the bipartite surroundings of the cluster on the substrate.

Secondly, the shape of the cluster after collision at the substrate is not perfectly ellipsoidal because there is an extended size contact area between the cluster and the substrate which is flat. The axial ratio c/a therefore only roughly describes the overall shape of the cluster.

To a certain extent, these limits can be overcome if one calculates the optical spectra of clusters on a substrate by more sophisticated theories. Examples are the theory performed by Ruppin [13] for a spherical particle touching a substrate, and the theory by Wind et al. [14] for spheroidal particles or truncated spheres on a substrate. We will discuss later how the results of these calculations compare to our more simple model for the special case of our experimental results shown below.

2.3 Electromagnetic coupling among clusters

The former equations only hold if the particles are exited independently. This condition is fulfilled for low surface coverages. If this limit is surpassed, electromagnetic coupling among the clusters and finally, for still larger coverages, cluster–cluster coalescence occur [11]. These effects strongly alter the above described anisotropy of the optical absorption.

A simple model to describe the influence of the electromagnetic coupling for spheres using the quasistatic approximation is described, e.g., in [11, 15]. In the quasistatic approximation the absorption of a single spherical cluster can be described as due to a dipole exited by the external electric field. If there are other clusters nearby, forming cluster aggregates, the total electric field at a given cluster will result from the superposition of the external incident field and the dipole fields of all other clusters. In general, this leads to a splitting of the single particle resonance of (1) into several different resonances. An exact calculation of such electromagnetic coupling effects between spherical clusters, including retardation and higher multipoles, thus also applicable for larger clusters, is given in [16].

Electromagnetic coupling of the clusters is effective for cluster–cluster distances smaller than 5 times the cluster radius and may lead to complicated extinction spectra by splitting of the single cluster resonance which depends on size and shape of the formed cluster aggregates [16].

It is important to state that spectra of two-dimensional aggregates of spherical clusters on a substrate look similar to the $\perp$- and $\parallel$-polarisation spectra for single oblate spheroidal clusters. Therefore the two effects, non-spherical shapes of the clusters and electromagnetic coupling, are difficult to distinguish in the extinction spectra. A combination of ellipsoidal cluster shapes and electromagnetic coupling of the clusters has to be used for the description of the optical properties of silver island films [17].

For further increased coverages the clusters eventually get into contact and cluster–cluster coalescence occurs. Again, the spectra are changed drastically. If the coalescence areas are extended, this leads finally to optical spectra similar to those of thin metal films with large “metal” extinction at low frequencies.

If island films are produced by condensation of atoms on a substrate the cluster size and shape and the cluster coverage vary simultaneously. This leads to continuous changes of the features of the optical spectra. If, however, the clusters are pre-formed before deposition as in our experiments described below, optical extinction spectra for different cluster coverages differ only in a constant factor proportional to the coverage as long as the clusters are well separated. Therefore the axial ratio c/a can be determined directly from the corresponding spectra. For larger coverages electromagnetic coupling and, finally, coalescence render this straight forward evaluation impossible, as in the case of island films.

3 Results and discussion

The proposed method to determine cluster deformations by optical means was tested with silver clusters deposited on quartz glass substrates.

Free silver clusters in vacuum were produced by supersonic expansion of silver vapour, with a mean diameter of $2R$ = 2.0 nm (i.e. $\approx 3 \cdot 10^2$ atoms) and with a moderate size distribution (standard deviation $s_{2R} \approx 0.6\,nm$). Transmission electron microscopy (TEM) of the clusters, deposited on carbon foil covered TEM grids, was used to measure the cluster sizes. By restricting to extremely low cluster coverages of the order of 10^{11} clusters cm^{-2} we excluded coalescence on the TEM samples. For calculating $2R$ and s_{2R}, cubic averaging was used which is the apt way if optical absorption is concerned [11]. From gasdynamics, taking into account the parameters of the expansion in the cluster source [21], the cluster velocity in the free beam was calculated to $1.5 \cdot 10^3\,m\,s^{-1}$. The experimental setup is described elsewere [12, 18], it can be used for direct optical spectroscopy of the free cluster beam in vacuum and of the very same clusters after deposition or embedding. The cluster coverage was measured using a quartz crystal microbalance. For calibration the relation was applied that one dense-packed cluster monolayer corresponds to an effective silver film thickness of $1.2 \cdot R$. The optical extinction was measured in situ in vacuum, with $\perp$-polarized and with $\parallel$-polarized light in oblique incidence (θ = 70^o), for different coverages on the quartz glass substrate. The dielectric constant of the quartz glass substrate is ε_{sub} = 2.15.

Spectra from coverages below 0.1 cluster-monolayers on a quartz glass substrate are plotted in Fig. 3. All spectra have similar shapes. They differ only in a constant factor proportional to the cluster coverage. This is checked in Fig. 3 by the dotted lines, which were produced by multiplication of the curve measured from 0.03 cluster-monolayers by the factors 2 and 3 accordingly, to fit to the measured spectra for 0.06 and 0.09 cluster-monolayers. The good correspondence with the according measured spectra proves that electromagnetic coupling, coalescence or rapid Ostwald ripening of the clusters can be neglected for cluster coverages below 0.1 cluster-monolayers on the quartz glass substrate. High coverages would have caused, instead, changes of the features of the spectra. Hence the optical spectra in Fig. 3 represent the absorption cross-section of well separated, isolated single clusters on the substrate.

In Fig. 4 the two measured polarization dependent spectra for a coverage of 0.06 cluster monolayers (see second curve in Fig. 3) are compared to calculated ones. Inserting the dielectric function $\varepsilon(\omega, R)$ of the clusters, which includes size and interface effects [12], in (2) and (4), $\sigma_{abs}^{\perp}$ $\sigma_{abs}^{\parallel}$ of Fig. 4 were computed. The two spectra measured in $\perp$- and $\parallel$-polarization were to be described by the same values for ε_m and c/a. So both parameters can be fitted unambiguously to the experiment. A change of ε_m shifts the energetic position of both peaks in the same direction, while the value of c/a determines the splitting of the peak positions. The thus evaluated parameters are ε_m = 1.48, L_a = L_b = 0.313 and L_c = 0.374. The latter results in an axial ratio c/a = 0.86 (a is the major axis parallel and c the minor axis perpendicular to the substrate). Because of the moderate peak splitting, the second peak in the spectrum for $\parallel$-polarization corresponding to σ_{abs}^{a} is only visible as a slight shoulder and shows no extra maximum.

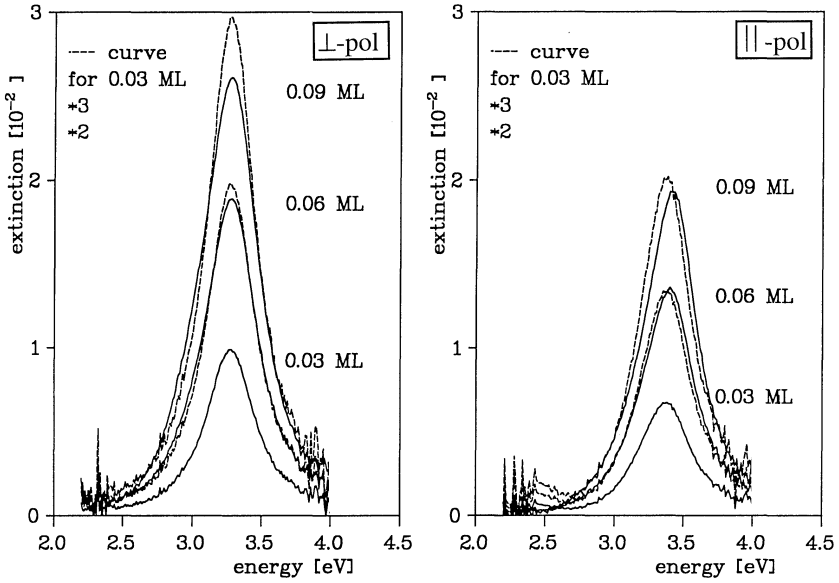

Fig. 3. Optical extinction spectra of silver clusters ($2\overline{R}$ = 2 nm) deposited on a compact quartz glass substrate with coverages less than 0.1 cluster monolayer (ML). Measurement with oblique incidence (θ = 70^o) in $\perp$-polarization (*left*) and $\|$-polarization (*right*). As a test for independent cluster absorption the measured curve for 0.03 ML was multiplied with the factors 2 and 3 (*dashed lines*) in order to compare with the spectra measured at higher coverages. The correspondence proves that the clusters are well separated below coverages of 0.1 ML

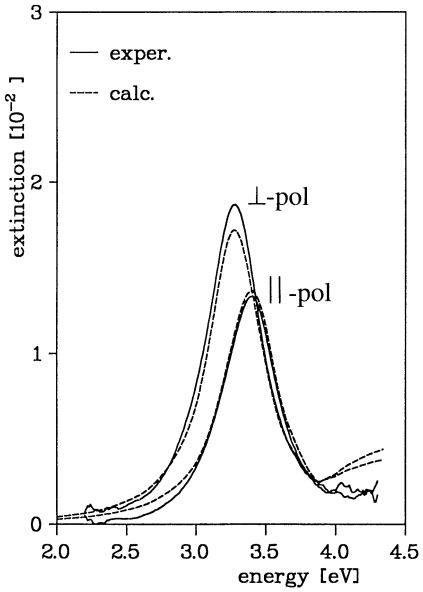

Fig. 4. Comparision between measured optical extinction spectra and calculated absorption cross-sections of spheroidal silver particles for a coverage of 0.06 cluster monolayer on a compact quartz glass substrate. Parameters of the model calculation: see text

The results of our model calculation will now be compared to the more sophisticated calculations decribed in [13] and [14].

One effect, missing in our model, is, that already a sphere touching a flat substrate shows some optical anisotropy. From the results of [13] it follows that the resonances of a sphere in vacuum touching a flat substrate with ε_{sub} = 2.31 shows an optical anisotropy which would be fitted corresponding to our model with a prolate spheroid (c/a = 1.08) embedded in a medium with ε_m = 1.18. Vice versa the calculations for spheroidal particles touching a substrate with ε_{sub} = 3.13 in [14] show a vanishing optical anisotropy for slightly oblate particles with c/a = 0.93. So, an application of these calculations to our experimental results would probably lead to an axial ratio c/a somewhat smaller than 0.86.

But there are other aspects which also have to be considered for the more detailed interpretation of our experimental results:

We already mentioned above that the shape of the deposited clusters is not perfectly ellipsoidal. As another model a truncated sphere was treated in [14]. The fit of the same experimental spectra assuming spheroidal particles or truncated spheres then resulted in significantly different axial ratios. Furthermore the size and interface dependence of $\varepsilon(\omega, R)$ not only influences the width of the cluster plasmon resonances, but there is also a moderate effect concerning the peak positions [22]. This, again, renders the precise evaluation of absolute peak positions difficult. However, the peak splitting caused by the optical anisotropy of the clusters on the substrate is less disturbed by these effects.

In summary, there are various refinements beyond our model calculation described above. But really getting more exact predictions of the cluster shape would be difficult. The essential result of the present investigation is that, in the given system, the collision induced cluster deformations are small, even for cluster velocities of $1.5 \cdot 10^3\, m\, s^{-1}$.

Apparently, there are not yet molecular dynamical simulations for the present system of silver clusters impinging on quartz glass substrates to compare with our obtained axial ratio data. The knowledge and manipulation of cluster deformations would be of practical importance, since it can be used for optimization of the cluster deposition for thin film production. We can compare our results with calculated data for similar systems if we accept that the parameter which mainly influences the deposition process is the kinetic energy per cluster-atom. The velocity of our clusters of $1.5 \cdot 10^3\, m\, s^{-1}$ corresponds to a kinetic energy of 1.3 eV per atom. Molecular-dynamics simulations for the deposition of metal clusters (Mo [1] or Cu, Ni and Al [3]) on a substrate of the same metal suggest that clusters of about $10^2 \ldots 10^3$ atoms stay almost spherical after the collision with a compact flat substrate for kinetic energies of 0.1 eV per atom, but they are completely destroyed when the kinetic energy

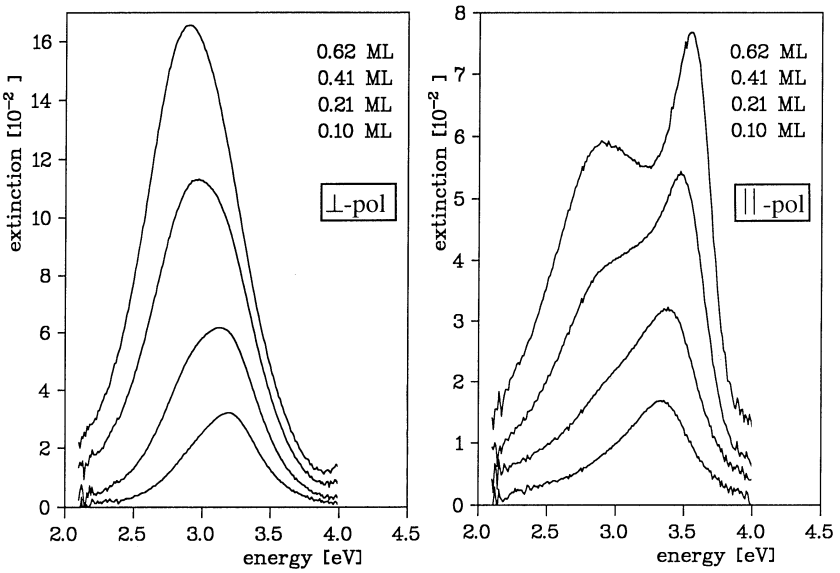

Fig. 5. Optical extinction spectra of silver clusters ($\overline{2R}$ = 2 nm) deposited on a compact quartz glass substrate with coverages larger than 0.1 cluster monolayer (ML). Measurement with oblique incidence (θ = 70^o) in ⊥-polarization (*left*) and ||-polarization (*right*). The coverage dependent changes of the shape of the spectra indicate that there is electromagnetic coupling among the clusters and coalescence to larger, unisometric silver islands

is 10 eV per atom. For an energy of about 1 eV per atom the calculations predict distinct deformation but no destruction of the clusters, which fits qualitatively to our experimental observations. It should be mentioned that in addition to the collision process also the surface- and interface-energies ("wetting"-effects) may give important contributions to the deformation of the cluster [8]. In molecular-dynamics simulations this is implied by the use of proper molecular interaction potentials.

Optical extinction spectra for coverages larger than 0.1 cluster-monolayers are plotted in Fig. 5. Here, with increasing coverage not only the magnitude but also the shape of the spectra change. In ⊥-polarization a strong shift to lower energies and a broadening of the cluster plasmon resonance can be observed, in ||-polarization the spectrum shows clearly two peaks.

The resonance peak for well separated clusters is Lorentzian on the low energy flank as follows from (2) with $\varepsilon(\omega)$ of silver, and was shown for example in Fig. 3. The deviations from the Lorentzian peak-shape observed, in contrast, in Fig. 5, occur because the extinction spectra consist of a superposition of different resonances. Possible reasons are coalescence to silver islands with variable shapes or the splitting into several different resonances because of electromagnetic coupling within a statistical distribution of small cluster-cluster distances. The high energy flank includes additional structure due to the interband absorption tail of silver at energies $\hbar\omega > 3.5$ eV. The interband absorption is included in the calculated spectra due to the use of the complete dielectric function of silver [19]. As following from Fig. 5, these effects are less sensitive to packing density.

The observation of electromagnetic coupling and coalescence which occur above certain cluster coverage is not surprising. But using optical spectroscopy to probe the deformation of the single, well separated clusters, it was important to avoid significant electromagnetic coupling and coalescence. Our experiments show that this is the case below a coverage of 0.1 cluster-monolayers. The direct observation of coverage dependent coalescence by usual TEM techniques was only possible by replacing the quartz glass substrate by thin carbon foils. So, it is important that, as we described above, the optical spectroscopy itself can be used to determine the onset of coupling and coalescence for the clusters.

4 Conclusion

Our experiments with fast silver clusters deposited with a velocity of $1.5 \cdot 10^3\, m\, s^{-1}$ on quartz glass substrates at room temperature showed that their collision-induced deformation can be measured in situ by polarization optics spectroscopy. The analysis of the optical cluster plasmon resonance excitation proved to be a sensitive tool for the determination of the resulting cluster shape and also of the arrangement of the clusters on the substrate.

We described the experimental method and a quantitative evaluation of our measured spectra. This yielded the axial ratio c/a = 0.86 of the well separated deposited clusters. Additionally, the coverage for the onset of electromagnetic cluster–cluster coupling and coalescence of the clusters on the substrate was determined to amount to 0.1 cluster monolayer.

We expect the presented method to be applicable more general to other cluster and substrate materials. Extended experiments with varied cluster velocities and substrate temperatures are being planned.

References

1. Haberland, H., Insepov, Z., Moseler, M.: Phys. Rev. B **51**, 11061 (1995)
2. Cleveland, C.L., Landman, U.: Science **257**, 355 (1992)
3. Hsieh, H., Averbeck, R.S., Sellers, H., Flynn, C.P.: Phys. Rev. B **45**, 4417 (1992)
4. Cheng, H.P., Landman, U.: Science **260**, 1304 (1993)
5. Fedrigo, S., Harbich, W., Buttet, J.: Phys. Rev. B **47**, 10706 (1993)
6. Vandoni, G., Félix, C., Goyhenex, C., Monot, R., Buttet, J., Harbich, W.: Surface Science **331–333**, 838 (1995)
7. Gatz, P., Hagena, O. F.: J. Vac. Sci. Technol. **A13**, 2128 (1995), Gatz, P., Hagena, O. F.: Appl. Surface Science **91**, 169 (1995)
8. Mahoney, W., Schaefer, D.M., Patil, A., Andres, R.P., Reifenberger, R.: Surface Science **316**, 383 (1994)

9. Relitzki, A., Hilger, A., Hövel, H., Kreibig, U., Schumacher, D., Winkes, H.: Science and Technology of Atomically Engineered Materials p 453. P. Jena, S.N. Khanna, B.K. Rao (eds.) Singapore: World Scientific 1996
10. Bohren, C.F., Huffman, D.R.: Absorption and Scattering of Light by Small Particles. Wiley: New York 1983
11. Kreibig, U., Vollmer, M.: Optical Properties of Metal Clusters, Springer Series in Material Science 25. Berlin Heidelberg: Springer 1995
12. Hövel, H., Fritz, S., Hilger, A., Kreibig, U., Vollmer, M.: Phys. Rev. B **48**, 18178 (1993)
13. Ruppin, R.: Surface Science **127**, 108 (1983)
14. Wind, M.M., Bobbert, P.A., Vlieger, J., Bedeaux, D.: Physica A **157**, 269 (1989)
15. Theiß, W. in: Festkörperprobleme/Advances in Solid State Physics 33. R. Helbig (ed), Vieweg, 1994, p 149
16. Quinten, M., Schönauer, D., Kreibig, U.: Z. Phys. D **12**, 521 (1989), Quinten, M., Kreibig, U.: Appl. Opt. **32**, 6173 (1993)
17. Normann, S., Anderson, T., Granqvist, C.G.: Phys. Rev. B **18**, 674 (1978)
18. Hövel, H.: Dissertation, RWTH Aachen 1995
19. Johnson, P.B., Christy, R.W.: Phys. Rev. B **6**, 4370 (1972)
20. Charlé, K.-P., Frank, F., Schulze, W.: Berichte Bunsengesellschaft Phys.Chem. **88**, 350 (1984)
21. Hagena, O. F.: Z. Phys. D **20**, 425 (1991)
22. Kreibig, U., Gartz, M., Hilger, A., Hövel, H. in: Science and Technology of Atomically engineered Materials p 403. J. Jena, S.N. Khanna, B.K. Rao (eds) Singapore: World Scientific 1996